Appl. Phys. B 79, 289–292 (2004)
DOI: 10.1007/s00340-004-1541-3

Applied Physics B
Lasers and Optics

S.O. KONOROV[1]
D.A. AKIMOV[1,2]
A.A. IVANOV[3]
E.E. SEREBRYANNIKOV[1]
M.V. ALFIMOV[3]
K.V. DUKEL'SKII[4]
A.V. KHOKHLOV[4]
V.S. SHEVANDIN[4]
YU.N. KONDRAT'EV[4]
A.M. ZHELTIKOV[1,2,✉]

Spectrally and temporally isolated Raman soliton features in microstructure fibers visualized by cross-correlation frequency-resolved optical gating

[1] Physics Department, M.V. Lomonosov Moscow State University, Vorob'evy gory, 119992 Moscow, Russia
[2] International Laser Center, M.V. Lomonosov Moscow State University, Vorob'evy gory, 119992 Moscow, Russia
[3] Center of Photochemistry, Russian Academy of Sciences, Novatorov 7a, 117421 Moscow, Russia
[4] S.I. Vavilov State Optical Institute, St. Petersburg 199034, Russia

Received: 22 March 2004
Published online: 23 June 2004 •

ABSTRACT We study soliton phenomena accompanying the propagation of femtosecond Cr: forsterite-laser pulses through a microstructure fiber in the regime of efficient anti-Stokes frequency conversion. The dispersion of the fiber is designed in such a way as to minimize the group delay of the 1.25-μm pump and the Stokes pulse within the length of soliton pulse compression in the regime of anomalous dispersion. Spectrally and temporally isolated solitonic features, resulting from soliton self-frequency shift, are detected at the output of such a microstructure fiber by means of cross-correlation frequency-resolved optical gating.

PACS 42.65.Wi; 42.81.Qb

1 Introduction

Microstructure (MS) fibers [1, 2] offer new strategies for the optimization of fiber-optic components and allow observation of new physical phenomena [3]. Dispersion tunability [4, 5], strong confinement of the light field in a small fiber core [6, 7], and large interaction lengths [8] attainable with MS fibers lead to a radical enhancement of nonlinear-optical processes [3], resulting in highly efficient supercontinuum generation [9, 10], which suggests convenient schemes of high-power pulse compression [11] and allows observation of interesting solitonic effects [4, 12, 13].

Similar to solitary waves in standard fibers [14], solitons in MS fibers experience a self-frequency shift [15, 16], induced [17, 18] by the Raman amplification of the low-frequency part of the soliton spectrum with a simultaneous depletion of the high-frequency wing of the spectrum. Dispersive waves emitted by frequency-shifted solitons contribute to efficient supercontinuum generation in MS fibers [12]. A negative dispersion slope, attainable with a certain design of MS fibers, has been shown recently [13] to lead to a new phenomenon of soliton self-frequency cancelation. Soliton self-frequency shift in MS fibers has been earlier intensely studied in the context of supercontinuum generation [19]. Dudley et al. [20] have applied cross-correlation frequency-resolved optical gating (XFROG) to analyze the evolution of supercontinua in MS fibers as a function of time and propagation coordinate.

✉ Fax: +7-095/9395-174, E-mail: zheltikov@top.phys.msu.su

In this paper, we focus on soliton effects in MS fibers designed for an efficient frequency up-conversion of ultra-short laser pulses through the generation of isolated anti-Stokes components [21]. This regime of nonlinear-optical spectral transformations of femtosecond pulses in MS fibers differs in its physical scenarios from the regime of supercontinuum generation, although many basic nonlinear-optical processes, of course, contribute to both anti-Stokes frequency conversion and supercontinuum generation. As shown by earlier work, MS fibers optimized for efficient anti-Stokes frequency conversion can be employed as sources of frequency-tunable ultra-short pulses ideally suited for applications in photochemistry [22] and coherent nonlinear spectroscopy [23]. In the experiments presented in this paper, we use the XFROG technique to study soliton phenomena accompanying the propagation of femtosecond Cr: forsterite-laser pulses through an MS fiber in the regime of efficient anti-Stokes frequency conversion. These measurements reveal spectrally and temporally isolated solitonic features arising in the field at the output of the MS fiber as a result of soliton self-frequency shift.

2 Microstructure fibers and the laser setup

Fused-silica MS fibers used in our experiments had a core with a diameter of about 4.5 μm and a cladding consisting of two cycles of air holes [8] (see inset in Fig. 1a). To model the properties of waveguide modes in such fibers, we employed a modification of the approach proposed by Monro et al. [24, 25], which involves a numerical solution [26, 27] of Maxwell's equations for the electric field in the cross section of an MS fiber. Figure 1a and b illustrate dispersion properties and present typical field intensity profiles for the fundamental and higher-order guided modes in these fibers. The fundamental mode is a doublet of degenerate modes with electric-field intensity reaching its maximum at the center of the fiber core

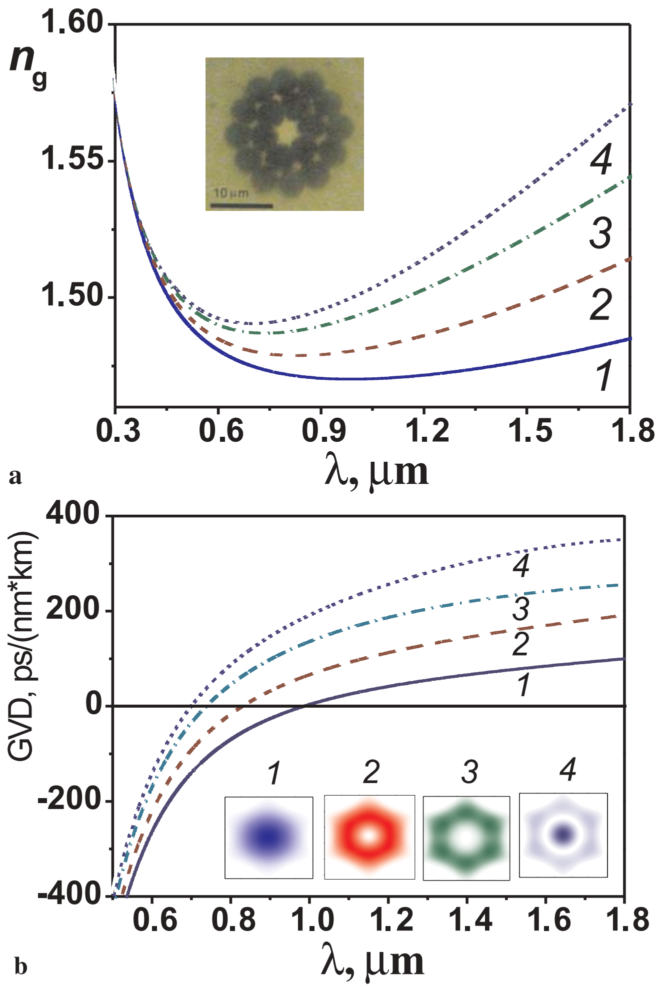

FIGURE 1 **a** The group index and **b** the group-velocity dispersion (GVD) calculated as functions of the wavelength for the fundamental (1) and higher-order (2–4) guided modes of the microstructure fiber with a core diameter of 4.5 μm (shown in the *inset* to (**a**)). Intensity profiles for the guided modes of the MS fiber are shown in *insets* 1–4 to (**b**)

and monotonically decreasing with the distance from the center of the fiber (inset 1 in Fig. 1b). Higher-order modes form degenerate multiplets (insets 2–4 in Fig. 1b), with their superposition supporting [28] the full symmetry of the fiber (see inset in Fig. 1a), identified as C_{v6} in our case.

Dispersion of the waveguide modes in MS fibers was optimized for efficient anti-Stokes frequency conversion through phase-matched four-wave mixing [21]. The wavelength of pump pulses (1.25-μm fundamental radiation of a Cr: forsterite laser) falls within the range of anomalous dispersion for the fundamental waveguide mode of the MS fiber (Fig. 1b), allowing the formation of both pump and Stokes-shifted solitons. The wavelength dependence of the group index for the fundamental guided mode of the MS fiber (Fig. 1a) was engineered in such a way as to reduce the group delay between the 1.25-μm pump and the Stokes pulse within the length of soliton pulse compression in the regime of anomalous dispersion (see the discussion in Sect. 3).

The laser system employed in our experiments (Fig. 2) consisted of a Cr^{4+}: forsterite master oscillator, a stretcher, an optical isolator, a regenerative amplifier, and a compressor. The master oscillator, pumped with a fiber ytterbium laser, generated 30–50-fs light pulses with a repetition rate of 120 MHz. The central wavelength of this laser radiation was 1250 nm with a mean power of about 180 mW. These pulses were then transmitted through a stretcher and an isolator to be amplified in an Nd:YLF-laser-pumped amplifier and recompressed to the 60-fs pulse duration with the maximum laser pulse energy up to 40 μJ at 1 kHz.

3 Results and discussion

Amplified pulses of a 1.25-μm Cr:forsterite laser were coupled into an MS fiber placed on a three-coordinate translation stage with a standard micro-objective. The initial duration of pump pulses at the input of the MS fiber was estimated as approximately 80 fs. MS fibers provided a 5% efficiency of frequency up-conversion of 50-nJ pump pulses to an anti-Stokes signal with a central wavelength of about 490 nm (see inset in Fig. 3a) through phase-matched parametric four-wave mixing. The wavelength of the anti-Stokes signal generated as a result of this process is dictated by phase matching and is controlled by the dispersion of the fiber [21].

Femtosecond pump pulses propagating in the MS fiber in the regime of anomalous dispersion tend to form high-order solitons [14]. The key features in the soliton evolution of the pump field are governed by the parameter $N = (L_d/L_{nl})^{1/2}$, where $L_d = \tau_0^2/|\beta_2|$ is the dispersion length (τ_0 is the initial pulse duration and $\beta_2 = \partial^2\beta/\partial\omega^2 = (\lambda^2|D|)/(2\pi c)$; β is the

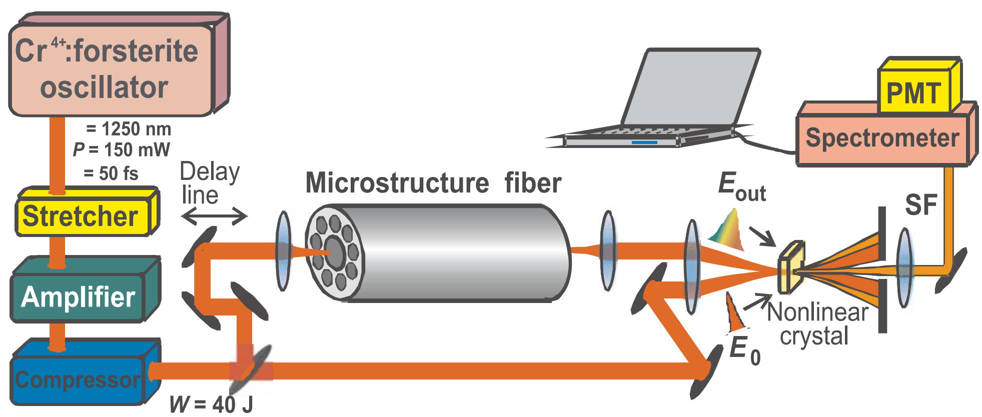

FIGURE 2 Diagram of the experimental setup for studying nonlinear-optical and solitonic effects accompanying the propagation of femtosecond laser pulses through a microstructure fiber: $\boldsymbol{E}_{out}$, signal transmitted through the MS fiber; $\boldsymbol{E}_0$, laser output; SF, sum-frequency signal; PMT, photomultiplier tube

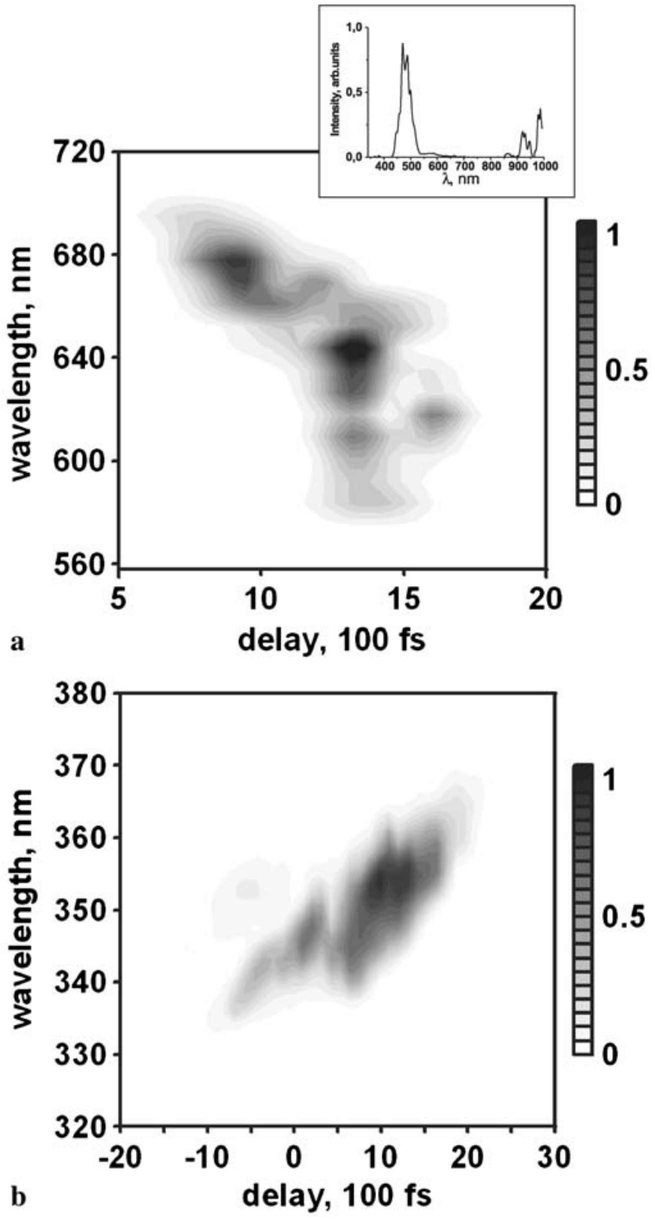

FIGURE 3 The intensity of the sum-frequency signal generated in a BBO crystal by a 70-fs pulse of 1.25-μm Cr : forsterite-laser radiation mixed with the pump transmitted through the MS fiber (**a**) and the anti-Stokes output of the MS fiber (**b**) as a function of the wavelength and the delay time τ between the Cr : forsterite-laser pulse and the signal at the output of the fiber. The fiber length is 5 cm. Laser pulses coupled into the MS fiber have an initial pulse duration of about 80 fs and an energy of 10 nJ. The *inset* in (**a**) illustrates anti-Stokes frequency conversion of 80-fs, 50-nJ Cr : forsterite-laser pulses, showing the visible part of the spectrum measured at the output of the MS fiber

propagation constant of a waveguide mode, ω is the radiation frequency, λ is the radiation wavelength, c is the speed of light, and D is the group-velocity dispersion (GVD), shown in Fig. 1b for MS-fiber modes) and $L_{\mathrm{nl}} = (\gamma P)^{-1}$ is the nonlinear length (P is the radiation power, $\gamma = (n_2\omega)/(cS_{\mathrm{eff}})$ is the nonlinear coefficient, n_2 is the nonlinear refractive index, and S_{eff} is the effective mode area). To estimate this parameter, we employ the results of calculations performed with the use of the above-described vectorial model of MS-fiber modes (Fig. 1b), yielding $|\beta_2| \approx 400\,\mathrm{fs}^2/\mathrm{cm}$. The dispersion length for pulses with an initial duration $\tau_0 \approx 80$ fs is thus $L_{\mathrm{d}} \approx 16$ cm. Estimating the effective diameter of the fundamental mode in the MS fiber (inset 1 in Fig. 1b) as $d_{\mathrm{eff}} \approx 4$ μm, we find that the nonlinear length for 80-fs, 10-nJ pulses is $L_{\mathrm{nl}} \approx 0.7$ mm, which gives $N \approx 15$.

High-order solitons, arising under our experimental conditions, display a periodic evolution behavior, going through the pulse-narrowing phase at the beginning of each cycle, splitting into several spikes, and merging again to recover the original shape at the end of the soliton period. The characteristic period of this oscillatory behavior is [14] $z_0 = (\pi L_{\mathrm{d}})/2 \approx 25$ cm. The optimum length for soliton compression, i.e. the length at which the central, solitonic spike of the pulse propagating through the fiber has a minimum width, is estimated as [29] $z_{\mathrm{opt}} \approx (0.32N^{-1} + 1.1N^{-2})z_0 \approx 0.7$ cm.

The key requirement for the efficient generation of Raman solitons is that the walk-off length for the pump and Stokes pulses, $L_{\mathrm{w}} = \tau_0 c|n_{\mathrm{gp}} - n_{\mathrm{gs}}|^{-1}$, where n_{gp} and n_{gs} are the group indices for the pump and Stokes pulses, should not be too small compared with the length z_{opt}. Dispersion of an MS fiber should, therefore, be designed in such a way as to minimize the group delay between the pump and Stokes pulses within z_{opt}. With the group-index mismatch for the pump and Stokes pulses propagating in the fundamental mode of our MS fiber $|n_{\mathrm{gp}} - n_{\mathrm{gs}}| \approx 10^{-3}$ (Fig. 1a), the walk-off length is estimated as $L_{\mathrm{w}} \approx 2.4$ cm. We have thus arrived at the following hierarchy of spatial scales of soliton evolution in our MS fibers: $L_{\mathrm{nl}} < z_{\mathrm{opt}} < L_{\mathrm{w}} < L_{\mathrm{d}}$. These relations suggest the possibility of efficient Raman soliton generation under conditions of our experiments.

To visualize the solitonic behavior of Cr:forsterite-laser pulses propagating through the MS fiber, we employed an experimental technique based on cross-correlation frequency-resolved optical gating (XFROG) [20]. An XFROG signal was generated by mixing the signal transmitted through the fiber, E_{out}, with the 70-fs fundamental-wavelength output of the Cr:forsterite laser, E_0, in a BBO crystal. A two-dimensional XFROG sonogram,

$$S(\omega, \tau) \propto \left| \int_{-\infty}^{\infty} E_{\mathrm{out}}(t) E_0(t-\tau) \exp(-\mathrm{i}\omega t)\,\mathrm{d}t \right|^2 ,$$

was then plotted by measuring the XFROG signal as a function of the delay time τ between the pulses $E_{\mathrm{out}}(t)$ and $E_0(t-\tau)$ and spectrally dispersing the XFROG signal (Fig. 2). XFROG sonograms of the pump and anti-Stokes signal at the output of a 5-cm MS fiber are shown in Fig. 3a and b, respectively.

The XFROG trace shown in Fig. 3a for pump pulses with an input energy of about 10 nJ reveals distinct solitonic features in the signal transmitted through the MS fiber. Red-shifted Raman solitons are observed as well-resolved dark spots on the XFROG sonogram. The soliton with a higher frequency, as can be seen from Fig. 3, appears at the output of the fiber earlier than the lower-frequency soliton. This sequence of solitons is explained by the anomalous dispersion of the fundamental mode of the MS fiber in the studied spectral range (Fig. 1b). The minimum duration of Raman soliton peaks, estimated as approximately 140 fs, was observed in experiments with a 3-cm MS fiber.

An XFROG trace of the anti-Stokes signal, generated within the range of wavelengths from 450 to 510 nm (see inset in Fig. 3a), indicates a positive chirp of this pulse. This result correlates well with the behavior of the dispersion of MS-fiber modes, which becomes normal within the 450- to 510-nm wavelength range (Fig. 1b). Because of the group-velocity mismatch between the anti-Stokes signal and the Raman solitons generated by the pump, solitonic features observed for the pump pulse cannot be directly mapped onto the anti-Stokes signal in our MS fibers. The temporal structure of the anti-Stokes signal is generally rather complicated under these conditions, as illustrated by the XFROG trace in Fig. 3b. This finding, in fact, suggests attractive strategies for the optimization of anti-Stokes frequency conversion of femtosecond pulses in MS fibers. It would be of special interest, in particular, to explore the ways of efficient frequency up-conversion of Raman solitons, formed in MS fibers by ultra-short pump pulses, through a phase- and group-velocity-matched four-wave mixing process.

4 Conclusion

We have presented the results of experimental studies of soliton phenomena accompanying the propagation of 1.25-μm femtosecond Cr: forsterite-laser pulses through microstructure fibers designed for efficient anti-Stokes frequency conversion. The walk-off length between the pump and Stokes pulses was minimized by engineering the dispersion of the fundamental mode of the MS fiber, thus providing optimal conditions for Raman soliton generation. Cross-correlation frequency-resolved optical gating, employed to characterize pulses transmitted through the MS fiber, has revealed spectrally and temporally isolated solitonic features in the output field, arising as a result of soliton self-frequency shift.

ACKNOWLEDGEMENTS We are grateful to A.B. Fedotov and D.A. Sidorov-Biryukov for their help and useful discussions.

This study was supported in part by a President of the Russian Federation Grant No. MD-42.2003.02, the Russian Foundation for Basic Research (Project Nos. 03-02-16929 and 02-02-17098), and INTAS (Project Nos. 03-51-5037 and 03-51-5288). The research described in this publication was made possible in part by Award No. RP2-2558 of the US Civilian Research & Development Foundation for the Independent States of the Former Soviet Union (CRDF). This material is also based upon work supported by the European Research Office of the US Army under Contract No. 62558-03-M-0033.

REFERENCES

1 J.C. Knight, J. Broeng, T.A. Birks, P.St.J. Russell: Science **282**, 1476 (1998)
2 P.St.J. Russell: Science **299**, 358 (2003)
3 C.M. Bowden, A.M. Zheltikov: J. Opt. Soc. Am. B **19**, 9 (2002)
4 W.H. Reeves, J.C. Knight, P.St.J. Russell: Opt. Express **10**, 609 (2002)
5 W.H. Reeves, D.V. Skryabin, F. Biancalana, J.C. Knight, P.St.J. Russell, F.G. Omenetto, A. Efimov, A.J. Taylor: Nature **424**, 511 (2003)
6 N.G.R. Broderick, T.M. Monro, P.J. Bennett, D.J. Richardson: Opt. Lett. **24**, 1395 (1999)
7 A.B. Fedotov, A.M. Zheltikov, A.P. Tarasevitch, D. von der Linde: Appl. Phys. B **73**, 181 (2001)
8 D.A. Akimov, M. Schmitt, R. Maksimenka, K.V. Dukel'skii, Yu.N. Kondrat'ev, A.V. Khokhlov, V.S. Shevandin, W. Kiefer, A.M. Zheltikov: Appl. Phys. B **77**, 299 (2003)
9 J.K. Ranka, R.S. Windeler, A.J. Stentz: Opt. Lett. **25**, 25 (2000)
10 A.M. Zheltikov: Appl. Phys. B **77**, 2 (2003)
11 T. Südmeyer, F. Brunner, E. Innerhofer, R. Paschotta, K. Furusawa, J.C. Baggett, T.M. Monro, D.J. Richardson, U. Keller: Opt. Lett. **28**, 1951 (2003)
12 J. Herrmann, U. Griebner, N. Zhavoronkov, A. Husakou, D. Nickel, J.C. Knight, W.J. Wadsworth, P.St.J. Russell, G. Korn: Phys. Rev. Lett. **88**, 173 901 (2002)
13 D.V. Skryabin, F. Luan, J.C. Knight, P.St.J. Russell: Science **301**, 1705 (2003)
14 G.P. Agrawal: *Nonlinear Fiber Optics* (Academic, Boston, MA 1989)
15 W.J. Wadsworth, J.C. Knight, A. Ortigosa-Blanch, J. Arriaga, E. Silvestre, P.St.J. Russell: Electron. Lett. **36**, 53 (2000)
16 X. Liu, C. Xu, W.H. Knox, J.K. Chandalia, B.J. Eggleton, S.G. Kosinski, R.S. Windeler: Opt. Lett. **26**, 358 (2001)
17 E.M. Dianov, A.Ya. Karasik, P.V. Mamyshev, A.M. Prokhorov, V.N. Serkin, M.F. Stel'makh, A.A. Fomichev: JETP Lett. **41**, 294 (1985)
18 F.M. Mitschke, L.F. Mollenauer: Opt. Lett. **11**, 659 (1986)
19 W.J. Wadsworth, A. Ortigosa-Blanch, J.C. Knight, T.A. Birks, T.P.M. Mann, P.St.J. Russell: J. Opt. Soc. Am. B **19**, 2148 (2002)
20 J.M. Dudley, X. Gu, L. Xu, M. Kimmel, E. Zeek, P. O'Shea, R. Trebino, S. Coen, R.S. Windeler: Opt. Express **10**, 1215 (2002)
21 D.A. Akimov, E.E. Serebryannikov, A.M. Zheltikov, M. Schmitt, R. Maksimenka, W. Kiefer, K.V. Dukel'skii, V.S. Shevandin, Yu.N. Kondrat'ev: Opt. Lett. **28**, 1948 (2003)
22 S.O. Konorov, A.M. Zheltikov: Opt. Express **11**, 2440 (2003)
23 S.O. Konorov, D.A. Akimov, A.A. Ivanov, M.V. Alfimov, A.M. Zheltikov: Appl. Phys. B **78**, 565 (2004)
24 T.M. Monro, D.J. Richardson, N.G.R. Broderick, P.J. Bennet: IEEE J. Lightwave Technol. **17**, 1093 (1999)
25 T.M. Monro, D.J. Richardson, N.G.R. Broderick, P.J. Bennet: IEEE J. Lightwave Technol. **18**, 50 (2000)
26 E.E. Serebryannikov, A.M. Zheltikov: Laser Phys. **13**, 1339 (2003)
27 S.O. Konorov, E.E. Serebryannikov, A.M. Zheltikov, P. Zhou, A.P. Tarasevitch, D. von der Linde: Opt. Express **12**, 730 (2004)
28 M.J. Steel, T.P. White, C. Martijn de Sterke, R.C. McPhedran, L.C. Botten: Opt. Lett. **26**, 488 (2001)
29 E.M. Dianov, Z.S. Nikonova, A.M. Prokhorov, V.N. Serkin: Sov. Tech. Phys. Lett. **12**, 311 (1986)